Vibrational Circular Dichroism of A-, B-, and Z-Form Nucleic Acids in the PO_2^- Stretching Region

Lijiang Wang, Ligang Yang, and Timothy A. Keiderling
Department of Chemistry, University of Illinois at Chicago, Chicago, Illinois 60607-7061 USA

ABSTRACT Vibrational circular dichroism (VCD) spectra were measured for H_2O solutions of several natural and model DNAs (single and double strands, oligomers and polymers) in the B-form, poly(dG-dC)·poly(dG-dC) in the Z-form, and various duplex RNAs in an A-form over the PO_2^- stretching region. Only the symmetric PO_2^- stretch at ~1075 cm^{-1} yields a significant intensity VCD signal. Differences of the PO_2^- stretching VCD spectra found for these conformational types are consistent with the spectral changes seen in the base region, but no sequence dependence was seen in contrast to VCD for base modes. The B to Z transition is accompanied by an inversion of the PO_2^- VCD spectra, which is characteristic of the change in the helical sense of the nucleic acid backbone. A-RNAs give rise to the same sense of couplet VCD as do B-DNAs but have a somewhat different shape because of overlapping ribose modes. These PO_2^- VCD spectral characteristics have been successfully modeled using simple dipole coupling calculations. The invariability of the symmetric PO_2^- stretching mode VCD spectra to the base sequence as opposed to that found for the C=O stretching and base deformation modes is evidence that this mode will provide a stable indication of the DNA helical sense.

INTRODUCTION

Vibrational Circular Dichroism (VCD) has displayed a powerful potential for sensing conformational changes of biopolymers (Keiderling and Pancoska, 1993; Diem, 1991). One of the advantages of VCD is that structurally sensitive data can be obtained for several different spectrally resolved transitions arising from the distinct localized excitations in the molecule. In nucleic acids, for example, it is possible with VCD to probe the in-plane base deformation modes to reveal the interbase stereochemistry and stacking interactions, the phosphate PO_2^- stretches to monitor backbone stereochemistry, and the various sugar modes to analyze the ribose conformation.

Since the first paper on nucleic acid VCD published from this laboratory (Annamalai and Keiderling, 1987), most attention has been focused on studies of the C=O, C=N, and C=C base in-plane deformation modes (Gulotta et al., 1989; Zhong et al., 1990; Wang and Keiderling, 1992; Yang and Keiderling, 1993). The bases can be viewed as locally achiral, being predominantly planar aromatics, and as coupled with each other via stacking interactions. Earlier VCD results for the base-localized vibrational modes in nucleic acids were applied to characterize the A-, B-, and Z-forms and showed evidence for strong base stacking effects and some base-sequence dependence, and provided diagnostics for the associated conformational changes (Annamalai and Keiderling, 1987; Gulotta et al., 1989; Wang and Keiderling, 1992). The observed VCD spectra have been shown to have a high sensitivity to the helical handedness, for example, the B and Z (right- and left-handed helical, respectively) forms of poly(dG-dC)·poly(dG-dC) are characterized by opposite signed VCD patterns, a positive and a negative couplet, respectively, that are in each case centered over the most intense IR band resulting from an in-plane base deformation mode. In most cases (except for Adenine), these are predominantly composed of a C=O stretching motion. By contrast, there is only a small intensity difference is found between the B- and A-form VCD in this region (both are right-handed helices) in all of the DNAs we measured. Synthetic duplex RNA yields VCD very similar to that of A-DNA, which would be expected from the similarity of their structures, the nearly identical vibrational modes involved (base-centered), and the postulated dependence of the base deformation VCD on stacking interactions alone.

Because they result in extremely high dipolar intensity IR transitions, vibrations of modes arising from the phosphate-sugar backbones of nucleic acids have been extensively studied by infrared spectroscopy (Taillandier et al., 1985). Furthermore, they are distinctly different from and have little vibrational coupling with the base in-plane vibrations. For example, Pilet and Brahms (1972) developed a linear dichroism technique to estimate the dihedral angle of the PO_2^- group with respect to the helical axis from symmetric and antisymmetric PO_2^- stretching modes in films, which has been used in refinement of nucleic acid structures (Arnott and Hukins, 1972). In view of the important role that the sugar-phosphate backbone of the nucleic acid plays in the conformation-related functions of DNA such as protein-DNA and drug-DNA binding, it is reasonable to establish firmly the potential structural information that can be gained from VCD spectra of the polymeric backbone vibrational modes.

In comparison with the base stretching region, VCD measurements of sugar-phosphate backbone modes have lagged. The first VCD of PO_2^- stretching region modes were

Received for publication 8 July 1994 and in final form 16 September 1994.

Address reprint requests to Dr. Timothy A. Keiderling, Dept. of Chemistry [M/C 111], Univ. of Illinois at Chicago, 845 W. Taylor St., Chicago, IL 60607-7061. Fax.: 312-996-0431; E-mail: tak@uic.edu.

Dr. Wang's current address: Genetics and Biochemistry Branch, National Institute of Diabetes and Digestive and Kidney Diseases, National Institutes of Health, Bethesda, MD 20892.

0006-3495/94/12/2460/08 $2.00

reported for the RNA duplex, poly(A)·poly(U), and triplex, poly(A)*poly(U)·poly(U) (Yang and Keiderling, 1993). The difference in the VCD sign pattern seen for the base deformation modes in the spectra of these two helical species (duplex and triplex, respectively) is accompanied by a change in the relative intensity of two bands in the PO_2^- symmetric stretching region (~1087 cm^{-1}).

It is the intent of this paper, therefore, to characterize the backbone conformations of various forms using VCD and to compare the VCD spectra arising from the base structure and the backbone structure, to lead, eventually, to a correlation of VCD spectral information and molecular structures. In this paper, we examine the VCD of B-DNA, Z-DNA and A-form RNA for the PO_2^- stretching modes and compare the experimental spectra with calculated spectra obtained using a simple dipole coupling model.

It is not possible for us to measure PO_2^- mode VCD for DNAs under the dehydrating conditions of very high alcohol concentration solution as was used in our previous work to study A-form DNA VCD because of spectral interference. Therefore, VCD of duplex RNA was used for the purpose of illustrating the difference in VCD between B-, A-, and Z-forms in the PO_2^- region, with care taken to identify the differences in the spectra caused by the effects of the ribose changes. Justification for this analogy comes from the similarity of A-RNA and A-DNA structures as evidenced by x-ray diffraction data and some spectroscopic results. Both structures have the same numbers of residues per turn (Arnott and Hukins, 1972), the same sugar pucker (C3′-endo), and a similar base-stacking arrangement and are generally assumed to be conformationally isomorphous (Saenger, 1984). DNA-RNA hybrids always adopt A-conformations common to both A-DNA and duplex RNA. Infrared linear dichroism indicates that not only the frequencies, but also the general sense of the polarization of the antisymmetric and symmetric PO_2^- stretching bands are virtually the same for A-RNA and A-DNA, being polarized perpendicular and parallel, respectively. Dihedral angles of both dipole moments with respect to the axis have been calculated from infrared dichroism (Pilet and Brahms, 1973) to be 70° and 40° for A-RNA and 65° and 45° for A-DNA, but are 56° and 70° for B-DNA for the antisymmetric and symmetric components of the PO_2^- stretch, respectively. Finally, VCD spectra of A-DNA and duplex A-form RNA in the base deformation region yield empirically consistent patterns in terms of both band shapes and intensities of the bands.

MATERIALS AND METHODS

Oligomers $d(pC\text{-}G)_2$ (lot 909–05A) and $d(pC\text{-}G)_3$ (lot 909–17A) and single-strand poly(C) (lot 13002) were obtained from Collaborative Research (Waltham, MA). Calf thymus DNA (lot 00544562), chicken blood DNA (lot 00424106), and poly(dG-dC)·poly(dG-dC) (QL82791002), poly(I)·poly(C) (lot 324723) were obtained from Pharmacia PLB (Milwaukee, WI). *Clostridium perfringens* DNA (lot 28F4008), *Micrococcus lysodeikticus* DNA (lot 68F4017), poly(dA)·poly(dT) poly(dA-dT)·poly(dA-dT) (lot 30H07121), yeast t-RNA (lot 47F-0751), and poly(A)·poly(U) (lot 88f-4005) were obtained from Sigma Chemical Co. (St. Louis, MO). Samples used for the first time were given no further treatment. Samples recovered from previous experiments by cleaning IR sample cells were dialyzed against 0.5–1 × 10^{-3} M NaCl and then were lyophilized in a SpeedVac (Savant Instrument, Inc., Farmingdale, NY). Spectra of B-form DNA and A-form RNA were obtained by dissolving those nucleic acids either in 0.1 M NaCl solutions or in 0.1 M NaCl and 10 mM Tris-HCl buffer to a final concentration of 30-~80 mg/ml. Z-form poly(dG-dC)·poly(dG-dC) was obtained by dissolving in 4.7 M NaCl. Unlike the other forms that are very viscous at high concentration, Z-form DNA in solution was quite fluid even at a concentrations as high as 60 mg/ml. Samples were placed in a home-made cell made of two BaF_2 windows separated by a 15 μ Teflon spacer that assured good transmittance in the spectral region down to 950 cm^{-1}.

All of the spectra were measured on the UIC dispersive VCD instrument, which has been described in the literature in detail (Keiderling, 1981, 1990). The slits of the monochromator were set at 8 mm wide and 30 mm high to achieve a high level of light throughput. This corresponds to a resolution of about 9 cm^{-1} at 1090 cm^{-1} using a 100 grooves/mm grating in our 1 m monochromator. Signal-to-noise ratio (S/N) was improved by averaging 4–8 scans. Equal numbers of scans of the baseline (same sample cell and path length with just buffer and H_2O) were collected and subtracted from the sample scans. These measurements were occasionally subject to artifacts in this region at certain frequencies such as 1170 cm^{-1}, which appeared to be sensitive to sample alignment and quality (fluidity). Control was possible through careful optical alignment and sample preparation and by checking all measurements with repeated scans of fresh sample preparations. Unless specified, to simplify comparison, all of the spectra presented here are normalized to a constant integrated absorbance of 30 cm^{-1} in the region of 1150–1020 cm^{-1} by curve-fitting the absorbance features in this region.

Model VCD calculations for the contributions caused by dipolar coupling were done using the Extended Degenerate Coupled Oscillator (EDCO) model put forth by Gulotta et al. (1989), which is based on the exciton model formalism (Tinoco, 1963) and was first applied to the VCD of dimers by Holzwarth and Chabay (1972). This model allows one to estimate a component of the rotational strength by assuming that the normal modes of interest can be represented by a localized transition dipole moment whose magnitude can be obtained from the measured absorption intensities of the corresponding monomer transitions. We have recently demonstrated that this model gives results that are consistent with the most accurate theoretical expressions for VCD when the dominant interaction between vibrational modes is dipolar coupling through space over substantial distances (Bour and Keiderling, 1992). The weak mechanical coupling between phosphate groups in a nucleic acid makes such modes an ideal test case for such a model of VCD. At the level considered here, only degenerate oscillators are considered, for which the rotational strength R^k and dipole strength D^k of the kth mode of an N dipole system are given by

$$R^k = -\left(\frac{\pi\nu}{c}\right)\sum_{i<j}^{N} C_{ik}C_{jk}\underline{\mathbf{T}}_{ij}\cdot\underline{\mu}_i\times\underline{\mu}_j$$

$$D^k = \sum_{i=1}^{N}\sum_{j=1}^{N} C_{ik}C_{jk}\underline{\mu}_i\cdot\underline{\mu}_j$$

where n is the unperturbed frequency of the dipole (in s^{-1}) and c is the speed of light. $\underline{\mathbf{T}}_{ij}$ is the distance from center of mass of dipole i to that of dipole j, $\underline{\mu}_i$ and $\underline{\mu}_j$ are the electric transition dipole moment vectors, and the coefficients C_{ij} are the elements of an eigenvector matrix $\mathbf{C}$. The eigenvectors ($\mathbf{C}$) result from diagonalizing the matrix of pairwise dipole-dipole coupling interactions. The calculations can be carried out on an empirical level, where the molecular vibrational transition frequency is the frequency of the monomer absorption maximum, and the magnitude of the electronic dipole moment is estimated from the experimental dipole strength. The geometries of A- and B-form DNA were obtained from coordinates provided with the Quanta software (Polygen, Durham, NC) and those of the Z-form from fiber x-ray data (Chandrasekaran and Arnott, 1989). The total dipole strength was estimated from integration of the corresponding absorption bands. A Gaussian function with a 20 cm^{-1} bandwidth was assumed in using the computed dipole and rotational strengths to simulate the spectra.

RESULTS

Typical PO_2^- region absorption and VCD spectra for a B-form deoxyribonucleic acid are given in Fig. 1 for calf thymus DNA (44% GC). The band at 1087 cm^{-1} is assigned to the symmetric stretching of PO_2^- and that at 1053 cm^{-1} to the C-O stretching in the ribose (Tsuboi, 1974). Corresponding to these absorption features, the VCD spectrum shows a sharp negative band at 1095 cm^{-1} and a broadened and less intense positive band to lower energy. From its frequencies and band shape, we can assign the strong positive VCD couplet (negative at 1095 and positive at 1075 cm^{-1}) to the symmetric PO_2^- mode. The sugar mode contributes added but weaker VCD overlapping the positive lobe of the couplet. The antisymmetric PO_2^- stretching band appears at 1224 cm^{-1} and gives no reliable VCD signal within our S/N and baseline limitations. The residual signals that are apparent in Fig. 1 are not reproducible when VCD spectra of separate samples are run. This latter observation holds for several RNA and DNA samples we measured, where no consistent patterns for the PO_2^- antisymmetric stretch were observed. Under the same conditions, the symmetric PO_2^- stretches yield consistent VCD spectra. We therefore conclude that the PO_2^- antisymmetric stretching does not generate useful VCD for conformational studies under our experimental conditions.

VCD spectra of double-stranded $(dG\text{-}dC)_2$, $(dG\text{-}dC)_3$, poly(dG-dC)·poly(dG-dC), and single-stranded poly(dC) are compared in Fig. 2. A distorted positive couplet is seen for all these synthetic DNAs as was seen in Fig. 1 for calf thymus DNA. The band intensities are enhanced in an unbalanced and nonlinear fashion as the chain length increases or bases are paired. There is a larger increase in the sharp negative band than in the flat positive band while the overall band shape remains qualitatively the same. Without its complementary strand, poly(dC) showed substantial helical structure consistent with a strong stabilization from the base-base interaction. This is consistent with base deformation VCD results measured for single-strand RNAs (Annamalai and Keiderling, 1987). The spectral change of the absorbance in this region is less dramatic than that of the VCD. As the 1087 cm^{-1} absorption band sharpens, the negative VCD band grows consistently more intense and sharp. The ribose C-O stretching band in single-strand poly(dC) is shifted to higher frequency (1060 cm^{-1}) from that in the double-strand examples (~1053 cm^{-1}) and is relatively more intense than that in double-stranded dG-dC. However, no VCD band shape change correlates to this absorption band alteration.

Another comparison is given in Fig. 3 for the double-stranded block copolymer poly(dA-dT) (*dashed line*) and the homopolymer poly(dA)·poly(dT) (*solid line*). Although

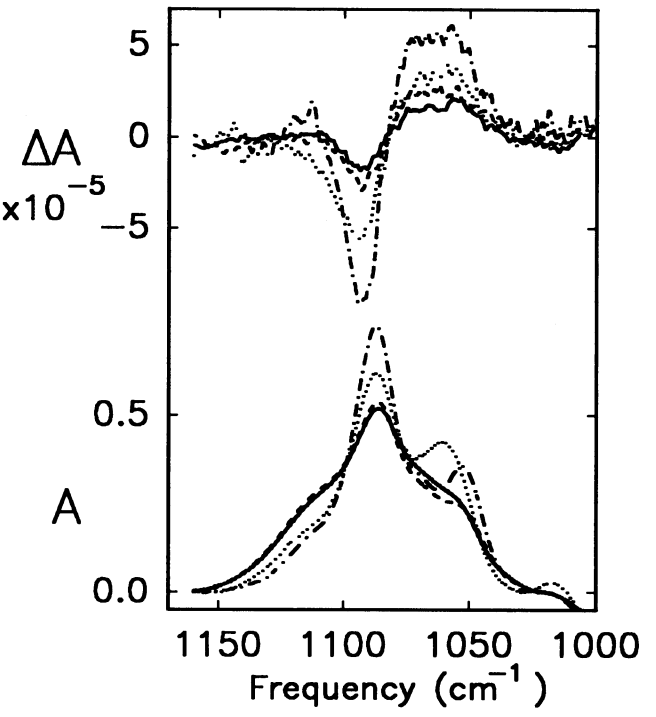

FIGURE 2 Comparison of the VCD and absorption spectra of $(dG\text{-}dC)_2$, $(dG\text{-}dC)_3$, poly(C), and poly(dG-dC)·poly(dG-dC). $(dG\text{-}dC)_2$: (——), 102 mg/ml; $(dG\text{-}dC)_3$: (- - - -), 87 mg/ml; poly(dC): (·····), 80 mg/ml; poly(dG-dC)·poly(dG-dC): (- · - · -), 30 mg/ml.

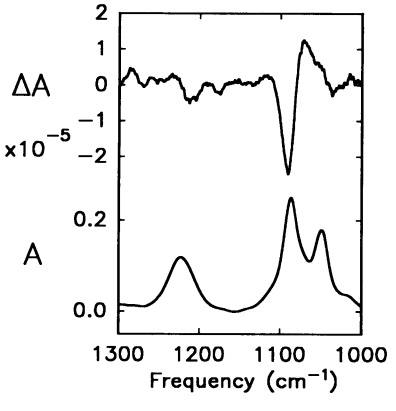

FIGURE 1 VCD and absorption spectra of calf thymus DNA (26 mg/ml) in the PO_2^- stretching region.

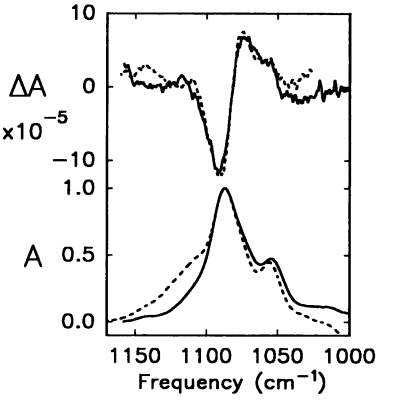

FIGURE 3 Comparison of the VCD and absorption spectra of B-form poly(dA-dT)·poly(dA-dT) (——) and B-form poly(dA)·poly(dT) (- - - -) in the PO_2^- stretching region. 10 mM Tris buffer at pH 7.0/H_2O, 28 and 50 mg/ml, respectively. Both VCD and absorption spectra were normalized to the 1087 cm^{-1} absorption peak.

their VCD and absorption spectra in the C=O stretching region differ from each other in both band shape and intensity (Zhong et al., 1990), their VCD and absorption spectra in the PO_2^- region are virtually identical, indicating that their PO_2^- conformations must be very much alike. Furthermore, these PO_2^- spectra for A-T model polymers are quite similar to those of the G-C models, having somewhat more pronounced positive PO_2^- VCD bands than seen for the dG-dC molecules in Fig. 2.

VCD spectra of B-form *c. perfringens* (28% GC) (*solid line*) and *m. lysodeikticus* (72% GC) (*dashed line*) DNA are shown in Fig. 4. Each DNA, with very different base contents, displays a negatively biased VCD spectral pattern similar to that seen in Figs. 1–3 for calf thymus DNA and the synthetic DNA polymers. Their absorption spectra are also similar, having a strong band at 1087 cm^{-1} and medium one at ~1053 cm^{-1}. Unlike the VCD of the base deformations (C=O stretch), these PO_2^- centered VCD spectra are shown to have little sequence dependence.

In Fig. 5 the VCD and absorption spectra of Z-form poly(dG-dC)·poly(dG-dC) (*solid line*) are compared, as induced by addition of 4.7 M NaCl, with the B-form result (*dashed line*). The high salt form is characterized by a negative couplet whose band shape over the PO_2^- mode is almost an inversion of the VCD spectrum of the B-form moiety. This comparison is clearer if one corrects for the positive contribution of the ribose mode at 1053 cm^{-1} in both cases. The 1087 cm^{-1} band in Z-form is much weaker relative to the 1053 cm^{-1} ribose C-O absorption band, which correlates to some loss in VCD intensity for the couplet. In between these prominent features lies an obvious shoulder band whose identity is unknown.

Fig. 6 *a* compares the VCD of synthetic A-form RNA poly(A)·poly(U) (*dashed line*) with that of B-form DNA poly(dA)·poly(dT) (*solid line*) for the symmetric PO_2^- mode. The 1120 cm^{-1} band in RNA arises primarily from C2′-O stretching, which apparently adds a second negative feature to the RNA PO_2^- VCD spectrum. To attain consistency with the DNA results, this band is excluded from the area normalization of the absorbance, which was therefore restricted

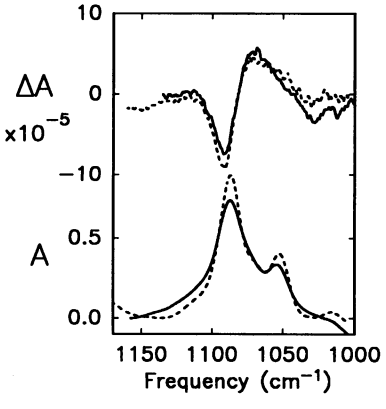

FIGURE 4 VCD and absorption spectra of B-form DNA from *m. lysodeikticus* (- - - -) and *c. perfringens* (——) in the PO_2^- symmetric stretching region. *m lysodeikticus*: 41 mg/ml; *c perfringens*: 30 mg/ml.

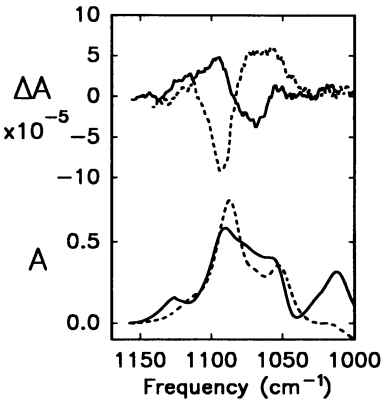

FIGURE 5 Comparison of VCD and absorption spectra of B-form and Z-form poly(dG-dC)·poly(dG-dC) in the PO_2^- stretching region. B-form (- - - - -): 30 mg/ml; and Z-form (——): 58 mg/ml.

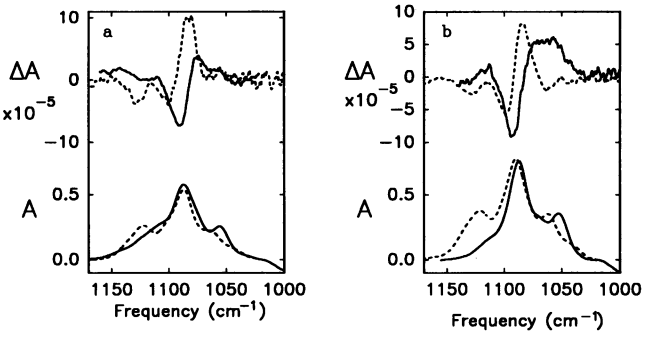

FIGURE 6 Comparison of VCD and absorption spectra between (*a*) B-form poly(dA)·poly(dT) (——, 28 mg/ml) and A-form poly(A)·poly(U) (- - - - -, 41 mg/ml) and (*b*) B-form poly(dG-dC)·poly(dG-dC) (——, 30 mg/ml) and A-form poly(I)·poly(C) (- - - -, 80 mg/ml) in the PO_2^- stretching region.

to the 1150–1020 cm^{-1} region. Although the symmetric PO_2^- stretching band is at almost the same frequency for both forms and both give rise to positive couplet VCD, the VCD spectra of the two forms (A and B) differ with respect to their zero crossing points and their different sense of bias (dominant sign, positive for RNA or negative for DNA). The same sort of the relationship can be seen by comparing the VCD of poly(I)·poly(C) and poly(dG-dC)·poly(dG-dC) (Fig. 6 *b*). The A-form antisymmetric stretching mode, again, showed no observable VCD signal (not shown). In an attempt to compare natural A and B form PO_2^- VCD, the spectra of yeast t-RNA, whose helical stems are in an A-form, are shown with that of chicken blood DNA in Fig. 7. The same patterns noted above for the synthetic models hold for these natural forms.

From these comparisons (Figs. 6 and 7), a general intensity pattern difference is seen with DNA having a strong negative band and RNA a strong positive band but both having a couplet of the same sense (deriving from the right hand helicity). This difference is accompanied by an up-shift of zero-crossing frequency to higher energy in the RNA. It might be that the extra band in the RNA absorbance spectrum is evidence of a positive couplet VCD centered on the 1120 cm^{-1}

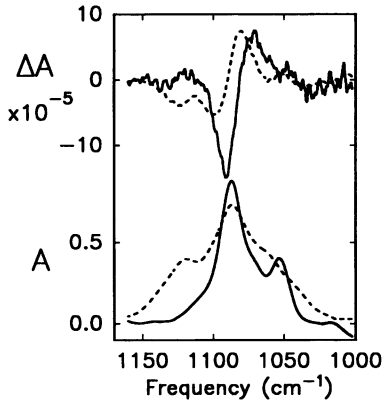

FIGURE 7 Comparison of VCD and absorption spectra between B-form chicken blood DNA (——, 58 mg/ml)and A-form yeast t-RNA (- - - -, 87 mg/ml) in the PO_2^- stretching region.

side band, which could lead to a weakening of the main negative feature at about 1100 cm^{-1}. This concept was tested, but it was not possible to fit satisfactorily the observed spectrum by assuming that the 1120 cm^{-1} absorption band corresponds to a positive couplet. Furthermore, the frequency shift of the zero crossing is the wrong direction if it were caused by overlap with a higher frequency couplet. No substantive intensity change in the negative peak results in such a test.

DISCUSSION

Both A-form RNA and B-form DNA give positive couplet VCD for the symmetric PO_2^- stretching mode. The small differences between them in terms of the bias sense of the couplets as well as the frequency up-shift of the RNA VCD couplet are not understood at present. Although these may derive from the difference in B and A forms, it is possible that the RNA result is significantly affected by the extra band deriving from the C-O stretches of the ribose.

By contrast, the Z-form VCD couplet in the PO_2^- stretching region reverses its sign with respect to the positive couplet given by A- and B-form. The same sense of sign reversal was seen in the C=O stretching region for a B-to-Z conformational change (Gulotta et al., 1989). Our results for the VCD of Z-form poly(dG-dC)·poly(dG-dC) in the C=O stretching region induced by either 80% TFE, 0.7 M $MgCl_2$, 4.7 M NaCl or even 2 M NaCl have all shown a reversed VCD sign pattern with respect to that of the right-handed B- and A-forms, as might be expected from the change of the helical sense between the B and Z forms (Gulotta et al., 1989; Keiderling et al., 1989; Wang and Keiderling, 1992, 1993; Birke et al., 1993). However, the Z form VCD in the base deformation region has a large frequency down shift and lower intensity as compared with the B form result, whereas in the PO_2^- region the change is predominantly one of sign pattern with some intensity loss. The consistency of the VCD changes in both regions for B-to-Z transitions further supports the conclusion that VCD is of value for sensing the helical handedness of nucleic acids.

The spectra of the B- and A-form DNAs in the 1550 to 1750 cm^{-1} region is strongly dependent on sequence or distribution of bases as illustrated in Fig. 8 by the comparison of VCD over that region for various B-form DNAs of differing compositions. The VCD spectra of the various duplex DNA polymers we studied in the PO_2^- region are similarly compared in Fig. 9. Considering that little coupling should occur between the base and phosphate groups, we did not expect and do not see a significant sequence dependence for the VCD of the symmetric PO_2^- stretching mode. This summary reflects our observations if only the 1087 cm^{-1} band is considered.

However, we do see a positive shoulder in the VCD at about 1070 cm^{-1} that has a small increase in intensity with increase in the GC content of these polymers. This correlates to development of a corresponding infrared absorption band for which an assignment is not available at present. Such a band has been suggested to be associated with the conformation of the sugar-phosphate groups and was suggested as an indicator of C-structure in poly(dA-dC)·poly(dG-dT) (Loprete and Hartman, 1989) and C and D structures in poly-(dA-dT)·poly(dA-dT) (Loprete and Hartman, 1990). It is possible that high A-T content causes some changes in the chain conformation, which is reflected by this spectral change. The sequence dependence of this 1070 cm^{-1} band in B-form DNA suggests some minor differences in the conformation of sugar-phosphate groups that could exist between G·C and A·T sequences.

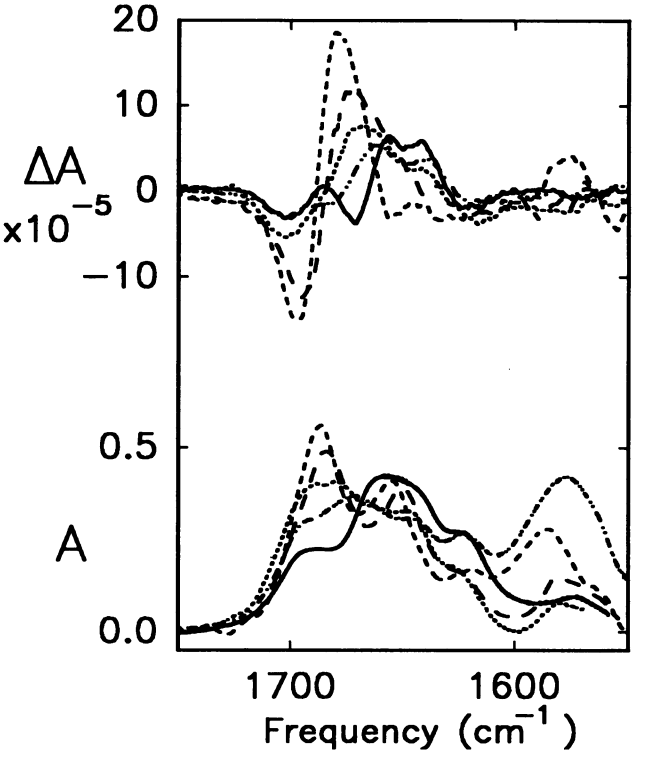

FIGURE 8 Sequence-dependent VCD and absorption of B-form DNA in C=O stretching region. (- - - - -): poly(dG-dC)·poly(dG-dC); (— — —): *m. lysodeikticus*, 72% GC; (·····): calf thymus, 44% GC; (- · - · -): *c. perfringens*, 26% GC; (——): poly(dA-dT)·poly(dA-dT).

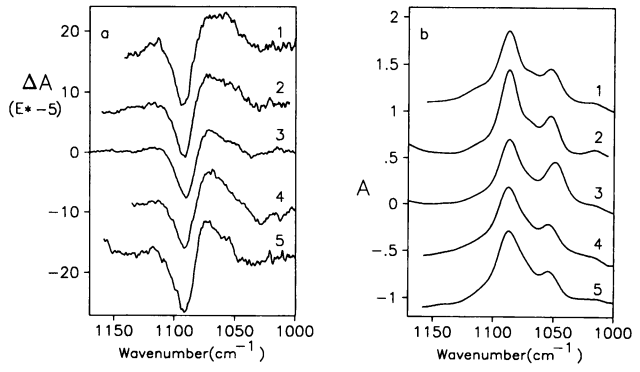

FIGURE 9 Sequence-independent VCD (*a*) and absorption (*b*) spectra of B-form DNA in the symmetric PO_2^- stretching region. 1: poly(dG-dC)·poly(dG-dC); 2: *m. lysodeikticus*, 72% GC; 3: calf thymus, 44% GC; 4: *c. perfringens*, 26% GC; 5: poly(dA-dT)·poly(dA-dT).

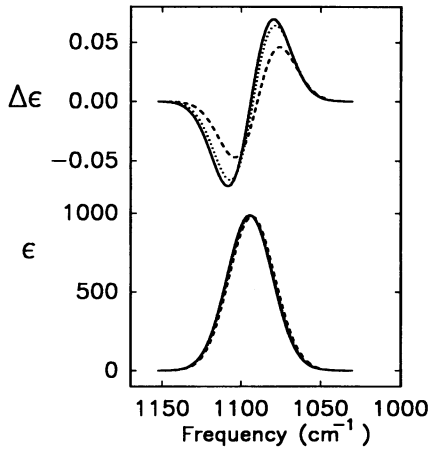

FIGURE 10 Computed VCD and absorption spectra of $(dG\text{-}dC)_2$ (- - - - -), $(dG\text{-}dC)_3$ (·····) and $(dG\text{-}dC)_5$ (——) for symmetric PO_2^- stretching. Spectra are normalized to per base and reproduced with Gaussian band shape with a HW = 20 cm^{-1}.

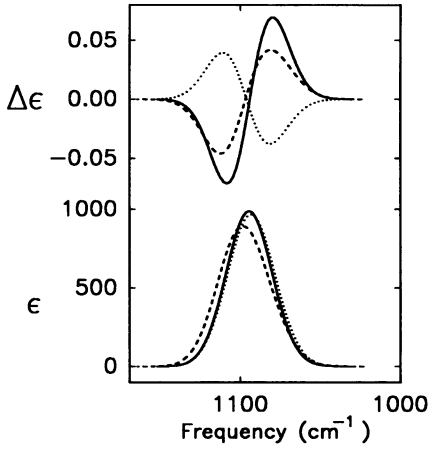

FIGURE 11 Computed VCD and absorption spectra of A-form (- - - - -), B-form (——), and Z-form (·····) $(dG\text{-}dC)_5$ for symmetric PO_2^- stretching. Spectra are normalized to per base and reproduced with Gaussian band shape with a HW = 20 cm^{-1}.

The sensitivity to the DNA sequence is thus different for base deformation and phosphate stretching VCD. Although the base-centered VCD is complicated by both the conformation and the heterogeneity of bases and offers more spectral diversity, the phosphate-stretching VCD is more independent and senses primarily the PO_2^- orientation. This level of specification for the origin of spectral features arising from two parts of the DNA molecule is simply not possible using more conventional electronic CD measurements that are not significantly affected by transitions associated with the PO_2^- groups.

A means of understanding these differences between A-, B-, and Z-form DNA VCD spectra can be obtained from a comparison of the results of extended degenerate coupled oscillator (EDCO) calculations (Gulotta et al., 1989; Holzwarth and Chabay, 1972) for these three structures with the experimental results. The dipole moments for symmetric and antisymmetric PO_2^- stretching transitions were modeled as lying along the bisector of the O-P-O angle and along a line connecting the two relevant O atoms, respectively (Tsuboi, 1974), and as having magnitudes derivable from the integrated absorbance spectra. The PO_2^- stretching modes are assumed to be locally achiral and isolated from other modes and from each other. Therefore, because they are also quite intense dipole oscillators, they serve as good model systems for EDCO calculation.

To compare with the experimental spectra, VCD and absorption spectra of $(dG\text{-}dC)_2$, $(dG\text{-}dC)_3$, and $(dG\text{-}dC)_5$ for the symmetric PO_2^- stretching mode were simulated (Fig. 10) using the EDCO formalism. The independence of the VCD band shape from effects of increase in the DNA chain length and the increase of the overall VCD intensity with increase in chain length is consistent with our experimental observations for oligomers (Fig. 2).

The bisignate VCD seen for A-form RNA and B- and Z-form DNA were simulated using the corresponding forms of $(dG\text{-}dC)_5$ (Fig. 11). Although the right-handed A-form VCD has the same sign pattern as right-handed B-form, the transition from B-form to a left-handed (Z-form) helix leads to an inversion of the VCD sign pattern and a decrease in the intensity of the VCD signal for the PO_2^- symmetric stretches. These computed spectra are exceptionally good matches to the experimental VCD results illustrated in Figs. 5 and 6 *b*. Calculations for the PO_2^- modes of A-form $(A)_{10}\cdot(U)_{10}$ yield the same results as for A-form $(dG\text{-}dC)_5$, in agreement with experimental results for the corresponding polymers. However, the shift of the A-form VCD couplet from the maximum absorption frequency, as seen in the experimental RNA PO_2^- VCD spectra, apparently is not explainable by simple dipole coupling of the PO_2^- modes.

The dominant mechanism for this observed PO_2^- VCD must be dipole coupling as seen from the excellent agreement of the results of these simple calculations with the experimental data. Comparison of the measured B-form chicken blood DNA and computed B-form $(dG\text{-}dC)_5$ VCD (Fig. 12) further shows that this agreement is not limited to one transition. The VCD from the antisymmetric as well as sym-

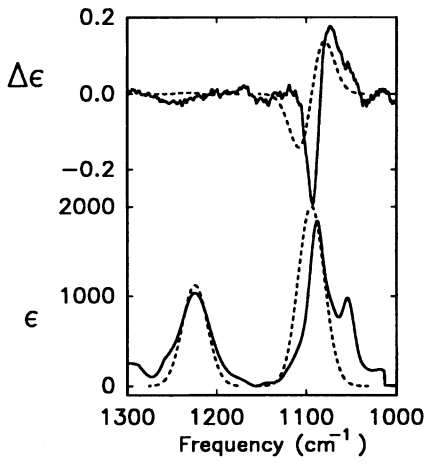

FIGURE 12 Comparison of calculated VCD and absorption spectra of B-form $(dG\text{-}dC)_5$ (- - - -) to the experimental results of chicken blood DNA (——) in the PO_2^- stretching region. Note: spectra are normalized to per base pair and reproduced with Gaussian band shape with a HW = 20 cm^{-1}.

metric PO_2^- stretches are properly represented in the calculations. The $\Delta A/A$ value for the antisymmetric PO_2^- stretch is calculated to be a factor of 45 smaller than for the symmetric PO_2^- stretch, resulting in a prediction of no observable VCD signal. Qualitatively the same calculational results were obtained for A-form $(dG\text{-}dC)_5$ for both modes. The distorted couplet band shape seen in the experimental VCD as compared with the conservative couplet seen in the theoretical VCD result is undoubtedly caused by mixing of local vibrational modes, which causes some intensity redistribution. However, the qualitative sense of the experimental VCD is clearly present in the theoretical result. The calculated VCD and absorption band shape and frequencies are found to be less sensitive to the dipole properties assumed for the symmetric PO_2^- stretch in the EDCO model than are those for C=O stretches. The well isolated PO_2^- dipoles and its well defined dipole moments probably account for the success of the EDCO model calculations in this case. Finally, it should be clear that the EDCO model is inherently sequence-independent, which is in agreement with our overall experimental observations but at the same time prevents it from addressing the subtler differences we have seen.

The overall result strongly supports the interpretation of the dominant features of the PO_2^- VCD as being caused by dipole-dipole coupling interactions. The coupled oscillator model additionally provides theoretical verification that VCD is indicative of the handedness of nucleic acids. Provided that the dipole geometry, the normal mode, and its frequency and intensity under all of the other influences except dipole-dipole coupling are known, the VCD and absorption spectra can be qualitatively predicted by the EDCO model for the base deformation region and for the PO_2^- stretching region. Conversely, given the VCD spectra and knowledge of the through-space coupled monomer transitions, the handedness of the helical twist can be determined unambiguously. The results for the PO_2^- modes are close to quantitative because of the modes involved being composed from relatively localized dipole oscillators and to their occurring in a less spectrally overlapped region.

CONCLUSION

In summary, we have shown that the VCD spectra of the phosphate-centered PO_2^- stretching mode is measurable for DNAs in H_2O solution and gives a band shape characteristic of the helical form. The VCD spectra in this region were shown to be relatively insensitive to base composition in contrast to the spectra measurable for the base deformation modes. The antisymmetric PO_2^- mode does not give reproducible VCD under our current sensitivity limits. The resulting spectra can be concluded to derive primarily from dipole coupling of the transition dipoles as judged by the success of our EDCO calculations in simulating the experimental results.

This work was supported by a grant from National Institutes of Health (GM 30147) for which we are most grateful.

REFERENCES

Annamalai, A., and T. A. Keiderling. 1987. Vibrational circular dichroism of poly(ribonucleic acids): a comparative study in aqueous solution. *J. Am. Chem. Soc.* 109:3125–3132.

Arnott, S., and D. W. L. Hukins. 1972. Optimized parameters for A-DNA and B-DNA. *Biochem. Biophys. Res. Commun.* 47:1504–1509.

Birke, S. S., M. Moses, B. Kagarlousky, D. Jano, M. Gulotta, and M. Diem. 1993. Infrared CD of deoxy oligonucleotides conformational studies of 5′d(CGCG)3′, and 5′d(GGCC)3′ in low salt and high salt aqueous solution. *Biophys. J.* 65:1262–1271.

Bour, P., and T. A. Keiderling. 1992. Computational evaluation of the coupled oscillator model in the vibrational circular dichroism of selected small molecules. *J. Am. Chem. Soc.* 114:9100–9105.

Chandrasekaran, R., and S. Arnott. 1989. The structures of DNA and RNA helices in oriented fibers. *In* Landolt-Bornstein New Series, Vol. 7. W. Saenger, editor. Springer-Verlag, Berlin. 104–170.

Diem, M. 1991. Solution conformation of biomolecules from infrared vibrational circular dichroism (VCD) spectroscopy. *SPIE Proc.* 1432:28–36.

Gulotta, M., D. J. Goss, and M. Diem. 1989. IR vibrational CD in model deoxyoligonucleotides: observation of the B-Z phase transition and extended coupled oscillator intensity calculations. *Biopolymers.* 28: 2047–2058.

Holzwarth, G., and I. Chabay. 1972. Optical activity of vibrational transitions: a coupled oscillator model. *J. Chem. Phys.* 57:1632–1635.

Keiderling, T. A. 1981. Vibrational circular dichroism. *Appl. Spectr. Rev.* 17:189–226.

Keiderling, T. A. 1990. Vibrational circular dichroism: comparison of techniques and practical considerations. *In* Practical Fourier Transform Infrared Spectroscopy. K. Krishnan and J. R. Ferraro, editors. Academic Press, San Diego. 203–284.

Keiderling, T. A., and P. Pancoska. 1993. Structural studies of biological macromolecules using vibrational circular dichroism. *In* Biomolecular Spectroscopy, Part B. R. J. H. Clark and R. E. Hester, editors. Wiley, Chichester. 267–315.

Keiderling, T. A., S. C. Yasui, P. Pancoska, R. K. Dukor, L. Yang, 1989. Biomolecular conformational studies with vibrational circular dichroism. *SPIE Proc.* 1057:7–14.

Loprete, D. M., and K. A. Hartman. 1989. Existence of the C structure in poly(dA-dC)·poly(dG-dC). *J. Biomol. Struct. Dyn.* 7:347–362.

Loprete, D. M., and K. A. Hartman. 1990. Conditions for the stability of the alternative structures of duplex poly(dA-dT). *Biopolymers*. 30:753–761.

Pilet, J., and J. Brahms. 1972. Dependence of B-A conformational change in DNA on base composition. *Nature*. 236:99–100.

Pilet, J., and J. Brahms. 1973. Investigation of DNA structural change by infrared spectroscopy. *Biopolymers*. 12:387–403.

Saenger, W. 1984. Principles of Nucleic acid structure. C. R. Cantor, editor. Springer-Verlag, New York. 253–282.

Taillandier, E., J. Liquier, and J. A. Taboury. 1985. Infrared spectral studies of DNA conformations. *In* Advances in Infrared and Raman Spectroscopy. R. J. H. Clark, and R. E. Hester, editors. Wiley Heyden, New York. 12:65.

Tinoco, I. 1963. The Exciton contribution to the optical rotation of polymers. *Radiat. Res.* 20:133–139.

Tsuboi, M. 1974. Infrared and Raman Spectroscopy. *In* Basic Principles in Nucleic Acid Chemistry. P. O. P. T'so, editor. Academic Press, New York. 399–452.

Wang, L. 1993. Vibrational circular dichroism studies of nucleic acid conformations. Ph.D. thesis. University of Illinois at Chicago.

Wang, L., and T. A. Keiderling. 1992. Vibrational circular dichroism studies of the A-to-B conformational transitions in DNA. *Biochemistry*. 31:10265–10271.

Wang, L., and T. A. Keiderling. 1993. Helical nature of poly(dI-dC)·poly-(dI-dC). Vibrational circular dichroism results. *Nucleic Acids Res.* 21: 4127–4132.

Yang, L., and T. A. Keiderling. 1993. Vibrational CD study of the thermal denaturation of poly(rA)·poly(rU). *Biopolymers*. 33:315–327.

Zhong, W., M. Gulotta, D. J. Goss, and M. Diem. 1990. DNA solution conformation via infrared circular dichroism: experimental and theoretical results for B-family polymers. *Biochemistry*. 29: 7485–7491.